High-Frequency Small-Signal Model of Ferrite Core Inductors

Marian K. Kazimierczuk, *Senior Member, IEEE*, Giuseppe Sancineto, Gabriele Grandi, Ugo Reggiani, *Member, IEEE*, and Antonio Massarini

***Abstract*— A circuit model of ferrite core inductors is presented. The behavior of the model parameters versus frequency is considered. The total power loss in inductors consisting of the winding resistance loss and the core loss, is modeled by a frequency-dependent equivalent series resistance. The total inductance given by the sum of the main inductance and the leakage inductance is obtained as a function of frequency. In order to study the core equivalent resistance and main inductance versus frequency, the magnetic field distribution in the core is derived from Maxwell's equations for a long solenoid. The complex permeability and permittivity of the ferrite core are introduced in the electromagnetic field equations. Experimental results are also given.**

***Index Terms*— Circuit modeling, coils, eddy currents, ferrite inductors, frequency response, magnetic cores, magnetic losses, skin effect.**

I. Introduction

ONE METHOD to reduce the overall size and weight of power converters is to increase the switching frequency above several hundred kilohertz. This allows the volume of inductors, capacitors, and transformers to be much smaller. To achieve this goal, it is important to obtain high efficiency at high operating frequencies. Moreover, parasitic components in the converter circuits must be accurately predicted to prevent unwanted behavior. The purpose of this paper is to explore the behavior of ferrite core inductors and present a circuit model valid at high frequencies in which parasitic capacitances, winding and core losses, and the frequency-dependent inductance are taken into account. Expressions are derived for the core equivalent resistance and main inductance as functions of frequency. The Dowell's equations [1] are used for the winding resistance and leakage inductance. Experimental results are also given.

II. Equivalent Circuit of Ferrite Core Inductors

Fig. 1(a) shows a lumped parameter model of a ferrite core inductor [2], [3], where R_w is the winding resistance, R_c is the core equivalent series resistance, $L_{\rm ac}$ is the total inductance, and C is the total parasitic capacitance. In general, R_w, R_c, and $L_{\rm ac}$ are dependent on frequency f. Fig. 1(b) shows the total ac resistance $R_{\rm ac} = R_w + R_c$. The impedance of the inductor model is $\hat{Z}_s = R_s + jX_s$. Fig. 1(c) depicts a series equivalent circuit of the inductor, where the equivalent series resistance (ESR) is [2], [3]

$$R_s = \frac{R_{\rm ac}}{(1-\omega^2 L_{\rm ac}C)^2 + (\omega C R_{\rm ac})^2} \tag{1}$$

and the equivalent series reactance is

$$X_s = \frac{\omega L_{\rm ac}\left(1 - \omega^2 L_{\rm ac}C - \dfrac{CR_{\rm ac}^2}{L_{\rm ac}}\right)}{(1-\omega^2 L_{\rm ac}C)^2 + (\omega C R_{\rm ac})^2} \tag{2}$$

where $\omega = 2\pi f$. Hence, the equivalent series inductance (ESL) is given by

$$L_s = \frac{X_s}{2\pi f} \tag{3}$$

which is also significant because most network analyzers and impedance meters measure R_s and L_s. The self-resonant frequency f_r of an inductor is defined as the frequency at which its reactance X_s becomes zero. Hence, from (2), the inductor total parasitic capacitance can be calculated as

$$C = \frac{1}{(2\pi f_r)^2 L_{\rm ac}(f_r) + \dfrac{R_{\rm ac}^2(f_r)}{L_{\rm ac}(f_r)}} \tag{4}$$

where $L_{\rm ac}(f_r)$ and $R_{\rm ac}(f_r)$ are the total inductance and total resistance at the resonant frequency f_r, respectively. The capacitance C is assumed to be independent of frequency.

III. Winding Resistance

The winding resistance of an inductor increases with frequency because of the skin and proximity effects due to the eddy current in the conductor generated by the time-varying electromagnetic field. The final result of these two combined effects is a reduction in the effective cross-sectional area of the wire available for the current flow. Therefore, the ac resistance at high frequencies becomes greater than the dc resistance. The winding ac resistance of an inductor with N_l layers is [1]

$$R_w = R_{w\rm dc} A\left[\frac{e^{2A} - e^{-2A} + 2\sin(2A)}{e^{2A} + e^{-2A} - 2\cos(2A)} + 2\frac{N_l^2 - 1}{3} \cdot \frac{e^{A} - e^{-A} - 2\sin A}{e^{A} + e^{-A} + 2\cos A}\right] \tag{5}$$

Manuscript received December 7, 1998; revised May 19, 1999.

M. K. Kazimierczuk and G. Sancineto are with the Department of Electrical Engineering, Wright State University, Dayton, OH 45435 USA (e-mail: mkazim@cs.wright.edu).

G. Grandi and U. Reggiani are with the Department of Electrical Engineering, University of Bologna, 40136 Bologna, Italy.

A. Massarini is with the Department of Engineering, Sciences University of Modena and Reggio Emilia, 41100 Modena, Italy.

Publisher Item Identifier S 0018-9464(99)08096-6.

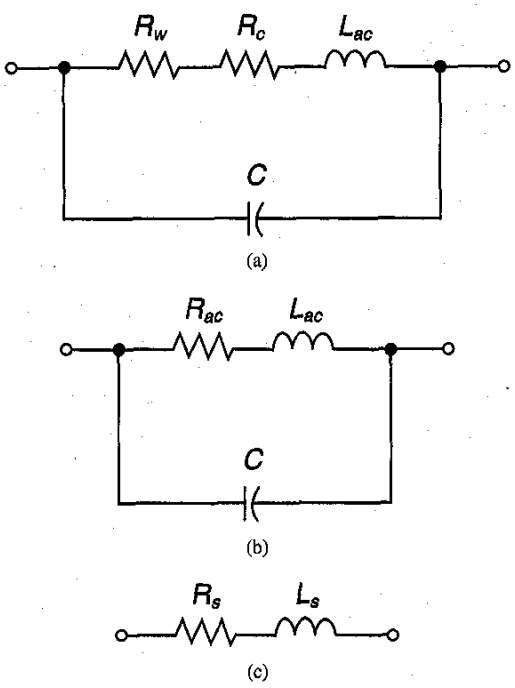

Fig. 1. Equivalent circuits of the inductor: (a) lumped parameter equivalent circuit, (b) equivalent circuit with $R_{ac} = R_w + R_c$, and (c) equivalent series circuit.

where R_{wdc} is the dc winding resistance at a given temperature T, and A for a round wire is

$$A = \left(\frac{\pi}{4}\right)^{3/4} \frac{d^{3/2}}{\delta t^{1/2}} \tag{6}$$

in which d is the conductor diameter, t is the distance between the centers of two adjacent conductors, and δ is the skin depth of the wire given by

$$\delta = \sqrt{\frac{\rho_w}{\pi \mu_0 \mu_{rw} f}}. \tag{7}$$

In (7), ρ_w is the wire resistivity ($\rho_w = 17.24 \times 10^{-9}$ Ωm for a copper wire at temperature of 20 °C), μ_{rw} is the relative magnetic permeability of the conductor material ($\mu_{rw} = 1$ for a copper conductor), and $\mu_0 = 4\pi \times 10^{-7}$ H/m.

IV. Main Inductance and Core Equivalent Resistance

Let us consider a coil uniformly wound around a ferrite core of length l and circular cross section of radius r_o. Assuming that the length of the cylindrical core is very long compared with its radius ($l \gg r_o$), edge effects can be neglected. Thus, the magnetic field can be considered uniform along the z axis of a cylindrical coordinate reference system, as shown in Fig. 2. Because of the cylindrical symmetry, the electric and magnetic fields are independent of φ and z coordinates. In particular, the magnetic field vector is given by

$$\boldsymbol{H}(r, \varphi, z, t) = H_z(r, t)\boldsymbol{a}_z. \tag{8}$$

For the sinusoidal steady state, we can introduce the magnetic field complex vector

$$\hat{\boldsymbol{H}}(r) = \hat{H}(r)\boldsymbol{a}_z \tag{9}$$

where the magnetic field phasor $\hat{H}(r)$ is given by

$$\hat{H}(r) = \hat{H}_z(r) = H_m(r)e^{j\alpha(r)}. \tag{10}$$

The present model takes into account the core magnetic hysteresis loss by a frequency-dependent complex magnetic permeability [4]

$$\hat{\mu}_c = \mu_o \hat{\mu}_{rc} = \mu_o(\mu'_{rc} - j\mu''_{rc}). \tag{11}$$

Therefore, the magnetic induction is described by a complex vector

$$\hat{\boldsymbol{B}} = \hat{\mu}_c \hat{\boldsymbol{H}} = \mu_o(\mu'_{rc} - j\mu''_{rc})\hat{\boldsymbol{H}}. \tag{12}$$

To take into account the core dielectric loss that occurs in grain boundary regions due to the electric hysteresis [4], [5], the electric permittivity is also expressed as a complex quantity dependent on frequency. Hence

$$\hat{\varepsilon}_c = \varepsilon_o \hat{\varepsilon}_{rc} = \varepsilon_o(\varepsilon'_{rc} - j\varepsilon''_{rc}). \tag{13}$$

The relationship between the electric displacement field complex vector $\hat{\boldsymbol{D}}$ and the electric field complex vector $\hat{\boldsymbol{E}}$ is given by

$$\hat{\boldsymbol{D}} = \hat{\varepsilon}_c \hat{\boldsymbol{E}} = \varepsilon_o(\varepsilon'_{rc} - j\varepsilon''_{rc})\hat{\boldsymbol{E}}. \tag{14}$$

In order to derive the main inductance and core equivalent resistance from the voltage induced across the winding by the time-varying magnetic flux, the magnetic field distribution in the core must be derived from Maxwell's equations. The Maxwell's equations in terms of complex vectors can be expressed as

$$\begin{aligned} \nabla \times \hat{\boldsymbol{H}} &= \hat{\boldsymbol{J}} + j\omega\hat{\boldsymbol{D}} \\ &= \gamma_c \hat{\boldsymbol{E}} + j\omega\hat{\varepsilon}_c\hat{\boldsymbol{E}} \\ &= (\gamma_c + j\omega\hat{\varepsilon}_c)\hat{\boldsymbol{E}} \\ &= \hat{\gamma}_c \hat{\boldsymbol{E}} \end{aligned} \tag{15}$$

$$\nabla \times \hat{\boldsymbol{E}} = -j\omega\hat{\boldsymbol{B}} = -j\omega\hat{\mu}_c\hat{\boldsymbol{H}} \tag{16}$$

where $\hat{\boldsymbol{J}}$ is the complex vector of the conduction current density, γ_c is the electric conductivity of the core, and $\hat{\gamma}_c = \gamma_c + j\omega\hat{\varepsilon}_c$ is its complex conductivity. In (15), $\gamma_c\hat{\boldsymbol{E}}$ is responsible of the eddy-current loss due to the nonzero conductivity γ_c of the core, $\omega\varepsilon_o\varepsilon''_{rc}\hat{\boldsymbol{E}}$ accounts for the dielectric loss, and the term $\omega\mu_o\mu''_{rc}\hat{\boldsymbol{H}}$ in (16) is related to the magnetic hysteresis loss. From (15) and (16), we can write

$$\nabla \times \left(\nabla \times \hat{\boldsymbol{H}}\right) = \hat{\gamma}_c \nabla \times \hat{\boldsymbol{E}} = -j\omega\hat{\mu}_c\hat{\gamma}_c\hat{\boldsymbol{H}} = -j\hat{k}^2\hat{\boldsymbol{H}} \tag{17}$$

where

$$\hat{k}^2 = \omega\hat{\mu}_c\hat{\gamma}_c. \tag{18}$$

From (9) and (17), it follows that

$$\frac{d^2\hat{H}}{dr^2} + \frac{1}{r}\frac{d\hat{H}}{dr} - j\hat{k}^2\hat{H} = \mathbf{0}. \tag{19}$$

This is the well-known Bessel's differential equation with the unique solution for $r \to 0$

$$\hat{H}(r) = GJ_0(j^{3/2}\hat{k}r) \tag{20}$$

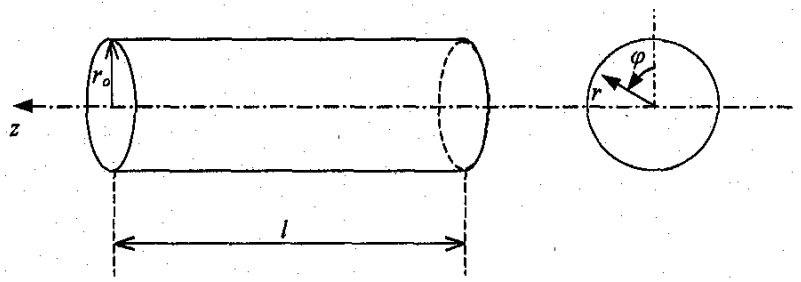

Fig. 2. Core geometrical view.

where J_0 is the Bessel's function of the first kind of zero order and G is an integration constant. Applying the boundary condition to the magnetic field phasor at the surface of the cylinder

$$\hat{H}_o = \hat{H}(r_o) = GJ_0\left(j^{3/2}\hat{k}r_o\right) \tag{21}$$

we can obtain

$$\hat{H}(r) = \hat{H}_o \frac{J_0\left(j^{3/2}\hat{k}r\right)}{J_0(j^{3/2}\hat{k}r_o)} \tag{22}$$

with

$$\hat{H}_o = \frac{N\hat{I}}{l} \tag{23}$$

where N is the total number of turns wound around the cylinder, and $\hat{I}$ is the phasor of the current in the coil. The magnetic flux phasor through a cross section is calculated as

$$\begin{aligned}\hat{\Phi} &= \int_S \hat{\mu}_c \hat{H}\, dS \\ &= 2\pi \int_0^{r_o} \hat{\mu}_c \hat{H}(r) r\, dr \\ &= \frac{2\pi\hat{\mu}_c\hat{H}_o}{J_0\left(j^{3/2}\hat{k}r_o\right)} \int_0^{r_o} rJ_0\left(j^{3/2}\hat{k}r\right) dr.\end{aligned} \tag{24}$$

Through the manipulations shown in the Appendix, (24) becomes

$$\hat{\Phi} = L_{\rm dc}^m \hat{I} \frac{2}{N} \frac{1}{\mu_o\mu'_{rc}} \frac{\hat{\mu}_c}{j^{3/2}\sqrt{2}\frac{r_o}{\hat{\delta}}} \frac{J_1\left(j^{3/2}\sqrt{2}\frac{r_o}{\hat{\delta}}\right)}{J_0\left(j^{3/2}\sqrt{2}\frac{r_o}{\hat{\delta}}\right)} \tag{25}$$

where $L_{\rm dc}^m$ is the low-frequency main inductance, J_1 is the Bessel's function of the first kind of order one, and $\hat{\delta}$ is given by (40). Neglecting the leakage flux, the magnetic flux linking the coil is

$$\hat{\Phi}_c = N\hat{\Phi}. \tag{26}$$

Hence, the voltage induced across the winding by the magnetic flux is

$$\hat{V} = j\omega\hat{\Phi}_c \tag{27}$$

and the impedance of the inductor is given by

$$\hat{Z} = \frac{\hat{V}}{\hat{I}} = j2\omega L_{\rm dc}^m \frac{1}{\mu_o\mu'_{rc}} \frac{\hat{\mu}_c}{j^{3/2}\sqrt{2}\frac{r_o}{\hat{\delta}}} \frac{J_1\left(j^{3/2}\sqrt{2}\frac{r_o}{\hat{\delta}}\right)}{J_0\left(j^{3/2}\sqrt{2}\frac{r_o}{\hat{\delta}}\right)}. \tag{28}$$

The real and imaginary parts of $\hat{Z}$ represent the core equivalent series resistance R_c (which accounts for the eddy current loss and both magnetic and electric hysteresis losses in the core) and the coil main reactance $\omega L_{\rm ac}^m$, respectively. These parameters are

$$\begin{aligned}R_{\rm c} &= {\rm Re}\left(\hat{Z}\right) \\ &= -\frac{4\pi}{\mu'_{rc}} f L_{\rm dc}^m\, {\rm Im}\left[\frac{\hat{\mu}_{rc}}{j^{3/2}\sqrt{2}\frac{r_o}{\hat{\delta}}} \frac{J_1\left(j^{3/2}\sqrt{2}\frac{r_o}{\hat{\delta}}\right)}{J_0\left(j^{3/2}\sqrt{2}\frac{r_o}{\hat{\delta}}\right)}\right]\end{aligned} \tag{29}$$

and

$$\begin{aligned}L_{\rm ac}^m &= \frac{{\rm Im}\left(\hat{Z}\right)}{2\pi f} \\ &= \frac{2}{\mu'_{rc}} L_{\rm dc}^m\, {\rm Re}\left[\frac{\hat{\mu}_{rc}}{j^{3/2}\sqrt{2}\frac{r_o}{\hat{\delta}}} \frac{J_1\left(j^{3/2}\sqrt{2}\frac{r_o}{\hat{\delta}}\right)}{J_0\left(j^{3/2}\sqrt{2}\frac{r_o}{\hat{\delta}}\right)}\right].\end{aligned} \tag{30}$$

V. Leakage and Total Inductances

An expression for the leakage inductance derived by Dowell [1] and simplified here is described by

$$L_{\rm ac}^l = R_{\rm wdc}\frac{A}{2\pi f}\left[\frac{e^{2A}-e^{-2A}-2\sin(2A)}{e^{2A}+e^{-2A}-2\cos(2A)} + 2\frac{N_l^2-1}{3} \cdot \frac{e^A-e^{-A}+2\sin A}{e^A+e^{-A}+2\cos A}\right]. \tag{31}$$

Thus, the total inductance of the coil is given by

$$L_{\rm ac} = L_{\rm ac}^m + L_{\rm ac}^l. \tag{32}$$

VI. Experimental Results

To verify the validity of the circuit model, an inductor was wound on a Siemens EC52 ferrite core (part no. B66341) with a circular cross section of the central leg and no air gap. This core uses N27 magnetic material. The diameter of the central

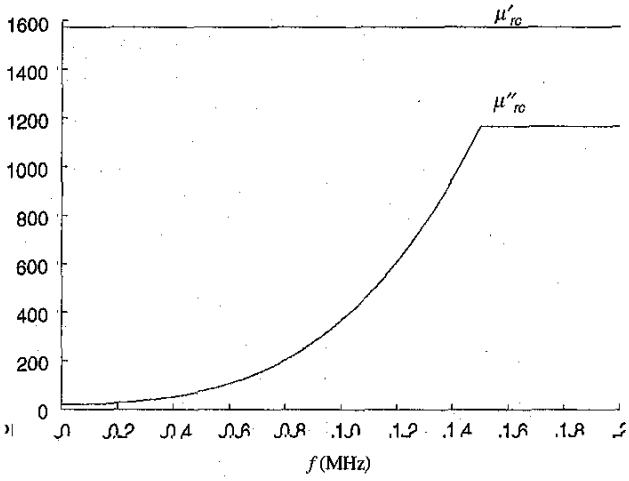

Fig. 3. Real part μ'_{rc} and imaginary part μ''_{rc} of the relative permeability of the Siemens N27 core material versus frequency.

leg was $2r_o = 13.75 \times 10^{-3}$ m. A solid copper wire with $d = 0.66 \times 10^{-3}$ m and $t \approx d$ (AWG#22) was wound on the central leg to obtain a one layer winding inductor ($N_l = 1$). The required number of turns of the winding inductor was $N_t = 39$. From data sheets, the inductance factor was $A_L = 3.4$ μH, resulting in the calculated low-frequency main inductance $L^m_{\rm dc} = (N_l N_t)^2 A_L = 5.15$ mH. The dc resistance calculated for the winding was $R_{w\rm dc} = 8\rho_w r_o N_t / d^2 = 84.89$ mΩ. The core resistivity was $\rho_c = 3$ Ωm. The measurements were performed using an HP 4194A impedance analyzer equipped with an HP 16047D test fixture [6] to achieve a higher accuracy by minimizing residual parameters such as lead inductances and contact resistances.

Using the data sheets in the Siemens catalogue, the real and imaginary parts of the complex permeability $\mu'_{rc}(f)$ and $\mu''_{rc}(f)$ for low values of magnetic induction B were approximated in the frequency range from 100 Hz to 2 MHz as shown in Fig. 3. The core ferromagnetic resonant frequency was about 2 MHz. Most inductors (except chokes) are operated well below the ferromagnetic resonance. For the tested core, the electrical hysteresis was neglected. Thus, only the real part of the relative permittivity was taken into account, so that $\hat{\varepsilon}_c = \varepsilon_o \varepsilon'_{rc}$. The core relative electric permittivity ε'_{rc} was calculated from measurements of a capacitance whose dielectric was a core material sample, using the same HP 4194A impedance analyzer. Fig. 4 shows the measured real part of the core relative permittivity by a dashed line, which was approximated by a solid line and used in computations. It can be seen that the real part of the permittivity decreases with frequency. In Fig. 5, the winding resistance R_w is plotted using the Dowell's equation (5). The winding resistance increased rapidly with frequency for $f > 20$ kHz. The equivalent series core resistance R_c given by (29) is plotted versus frequency in Fig. 6. As expected, the core resistance increased with frequency and reached very high values of the order of 40 kΩ. The main inductance $L^m_{\rm ac}$ versus frequency given by (30) is plotted in Fig. 7. The main inductance was independent of frequency up to 1 MHz and then rapidly decreased. At high frequencies, in spite of the ferrite low conductivity, eddy currents strongly weaken the magnetic field in the core and, consequently, the main inductance decreases. Fig. 8 shows the calculated and measured ESR R_s versus frequency.

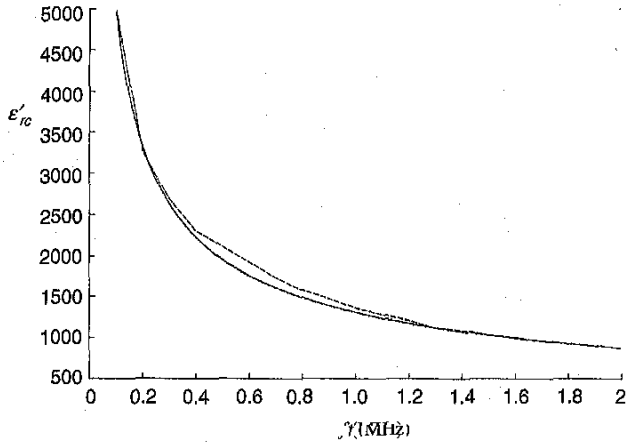

Fig. 4. Measured (dashed line) and approximated (solid line) relative permittivity ε'_{rc} of the Siemens N27 core material versus frequency.

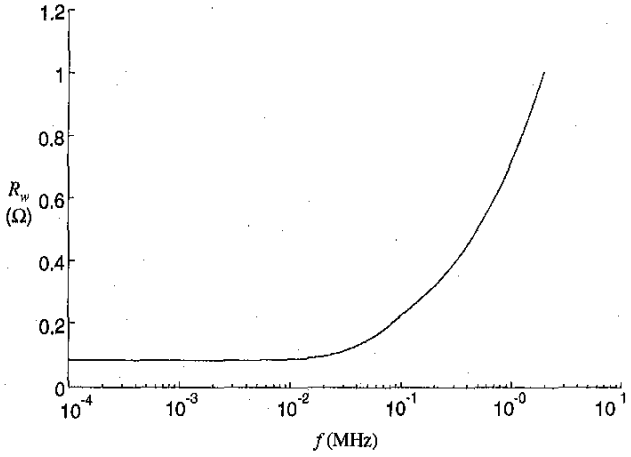

Fig. 5. Winding resistance R_w versus frequency.

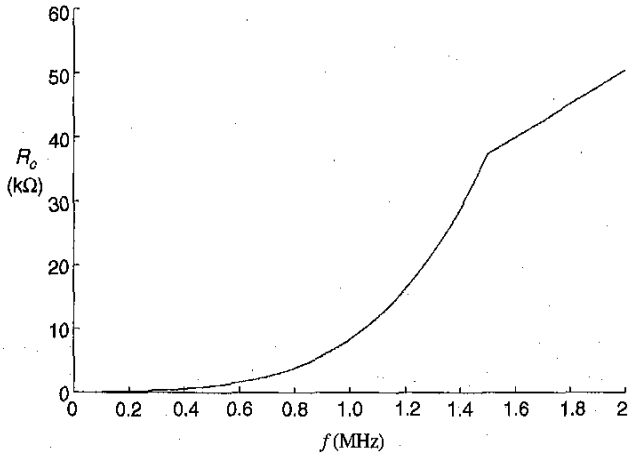

Fig. 6. Core equivalent series resistance R_c versus frequency.

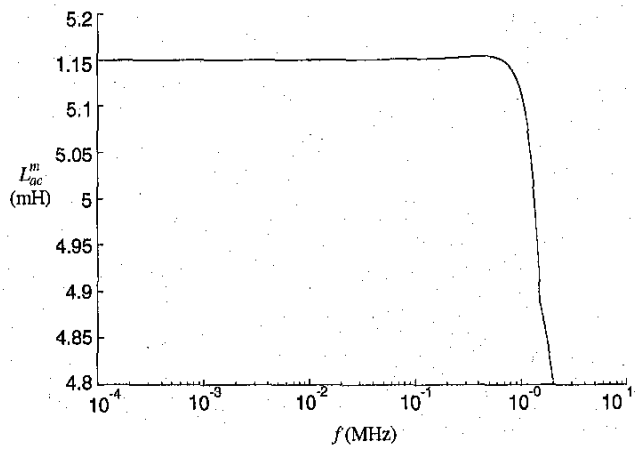

Fig. 7. Main inductance $L_{\rm ac}^{m}$ versus frequency.

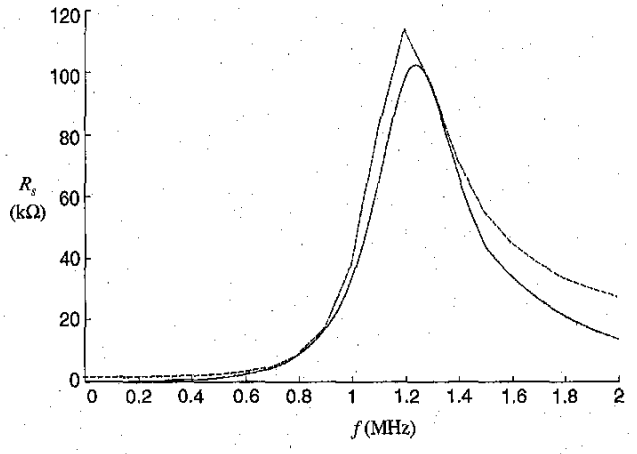

Fig. 8. Measured (dashed line) and calculated (solid line) ESR R_s versus frequency.

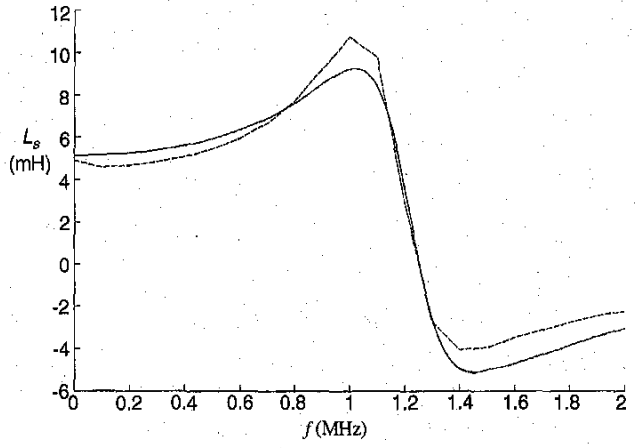

Fig. 9. Measured (dashed line) and calculated (solid line) ESL L_s versus frequency.

Fig. 9 depicts the calculated and measured ESL L_s versus frequency. In Fig. 10, the calculated and measured values of the magnitude of the inductor impedance are compared. Fig. 11 shows the behavior of the calculated and measured phase of the inductor impedance versus frequency. Fig. 12

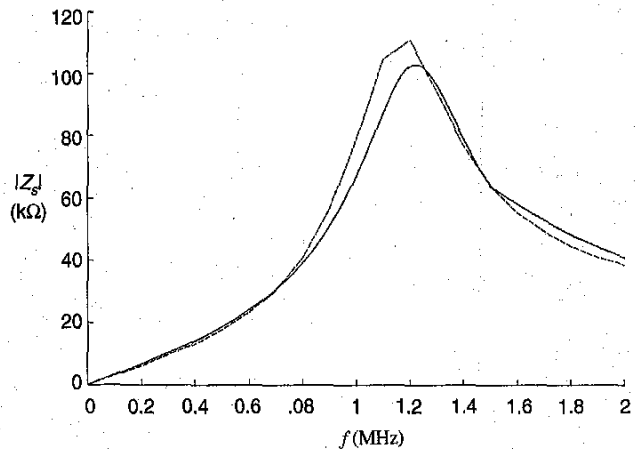

Fig. 10. Measured (dashed line) and calculated (solid line) magnitude of the inductor impedance $|Z_s|$ versus frequency.

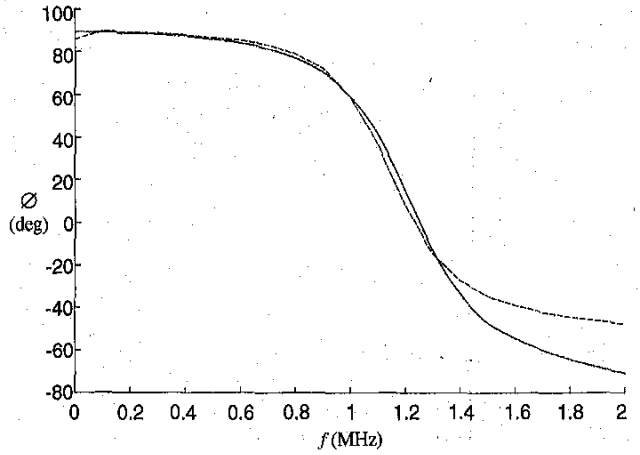

Fig. 11. Measured (dashed line) and calculated (solid line) phase of the inductor impedance ϕ versus frequency.

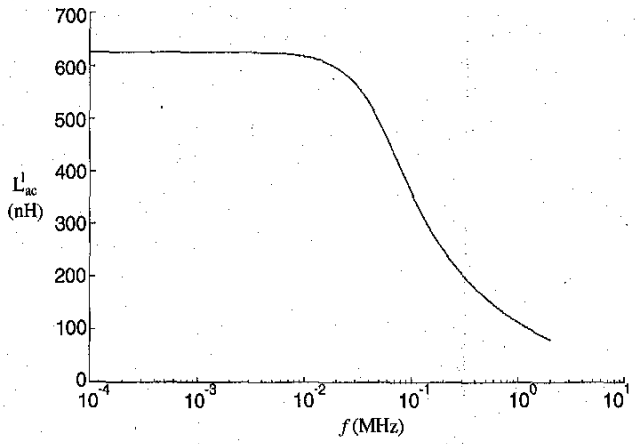

Fig. 12. Leakage inductance $L_{\rm ac}^{l}$ versus frequency.

shows a plot of the leakage inductance $L_{\rm ac}^{l}$ versus frequency. The leakage inductance is almost independent of frequency at low frequencies and decreases to zero at high frequencies. At high frequencies, the current tends to concentrate close

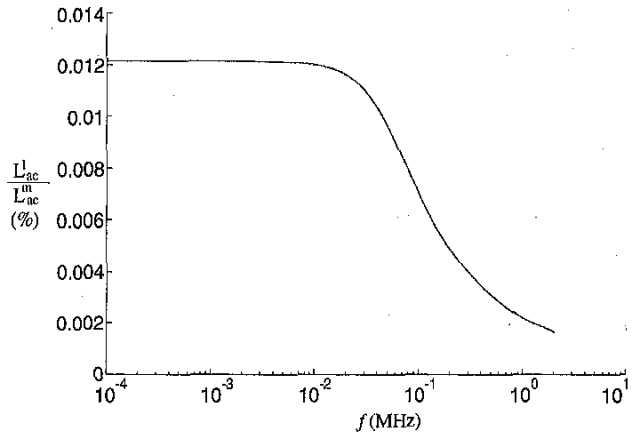

Fig. 13. Ratio of the leakage inductance to the main inductance L^l_{ac}/L^m_{ac} versus frequency.

to the surface of the conductor and the internal magnetic field approaches zero. The ratio L^l_{ac}/L^m_{ac} versus frequency is shown in Fig. 13. We can conclude that the leakage inductance is negligible as compared to the main inductance L^m_{ac} in the examined case of the ferrite core inductor with a single layer. For this reason, L^l_{ac} is neglected in this paper. The measured reactance was zero at $f = f_r = 1.25$ MHz. Hence, from (4) and Figs. 5–7, $C = 2.61$ pF was calculated. The choice of $N_l = 1$ in the experimental tests allows us to verify better the accuracy of the proposed formulas (29) and (30). In fact, (29) and (30) do not depend on the number of layers N_l, whereas Dowell's formula (5) and (31) do. Thus, it is desirable that the contributions of the winding resistance and leakage inductance given by (5) and (31) to the total ac resistance and inductance are reduced to a minimum. This minimum occurs when $N_l = 1$.

VII. Conclusion

A small-signal circuit model of ferrite core inductors has been examined and analytical functions have been derived to describe the behavior of the lumped parameters versus frequency. Experimental and calculated results have also been compared. It seems that the model is sufficiently accurate up to the self-resonance frequency. The model components are sensitive to the physical functions $\varepsilon'_{rc}(f)$, $\mu'_{rc}(f)$, and $\mu''_{rc}(f)$. A large-signal model is recommended for future research.

Appendix

Starting from (24), we can obtain (25) through the following manipulations. Letting

$$\hat{\eta} = j^{3/2}\hat{k} \tag{33}$$

$$\hat{\eta} r = \hat{v} \tag{34}$$

we can write

$$dr = \frac{d\hat{v}}{\hat{\eta}}. \tag{35}$$

Hence, the phasor of the magnetic flux through a cylindrical cross section given by (24) becomes

$$\begin{aligned}\hat{\Phi} &= 2\pi \frac{N\hat{I}}{l} \frac{\hat{\mu}_c}{J_0(\hat{v}_o)} \int_0^{\hat{v}_o} \frac{\hat{v}}{\hat{\eta}} J_0(\hat{v}) \frac{d\hat{v}}{\hat{\eta}} \\ &= 2\pi \frac{N\hat{I}}{l} \frac{\hat{\mu}_c}{J_0(\hat{v}_o)} \frac{1}{\hat{\eta}^2} \int_0^{\hat{v}_o} \hat{v} J_0(\hat{v})\, d\hat{v}. \end{aligned} \tag{36}$$

Using the Bessel's function property [7]

$$\int u^n J_{n-1}(u)\, du = u^n J_n(u) \tag{37}$$

(36) becomes

$$\begin{aligned}\hat{\Phi} &= 2\pi r_o^2 \frac{N\hat{I}}{l} \frac{\hat{\mu}_c \hat{v}_o}{\hat{\eta}^2 r_o^2} \frac{J_1(\hat{v}_o)}{J_0(\hat{v}_o)} \\ &= 2\pi r_o^2 \frac{N\hat{I}}{l} \frac{\hat{\mu}_c}{\hat{v}_o} \frac{J_1(\hat{v}_o)}{J_0(\hat{v}_o)} \\ &= L^m_{dc} \hat{I} \frac{2}{N} \frac{1}{\mu_o \mu'_{rc}} \frac{\hat{\mu}_c}{\hat{v}_o} \frac{J_1(\hat{v}_o)}{J_0(\hat{v}_o)} \\ &= L^m_{dc} \hat{I} \frac{2}{N} \frac{1}{\mu_o \mu'_{rc}} \frac{\hat{\mu}_c}{j^{3/2}(\omega \hat{\mu}_c \hat{\gamma}_c)^{1/2} r_o} \\ &\quad \cdot \frac{J_1\left[j^{3/2}(\omega \hat{\mu}_c \hat{\gamma}_c)^{1/2} r_o\right]}{J_0\left[j^{3/2}(\omega \hat{\mu}_c \hat{\gamma}_c)^{1/2} r_o\right]} \\ &= L^m_{dc} \hat{I} \frac{2}{N} \frac{1}{\mu_o \mu'_{rc}} \frac{\hat{\mu}_c}{j^{3/2}\sqrt{2}\frac{r_o}{\hat{\delta}}} \frac{J_1\left(j^{3/2}\sqrt{2}\frac{r_o}{\hat{\delta}}\right)}{J_0\left(j^{3/2}\sqrt{2}\frac{r_o}{\hat{\delta}}\right)} \end{aligned} \tag{38}$$

where the low-frequency main inductance is

$$L^m_{dc} = N^2 \frac{\mu_o \mu'_{rc} \pi r_o^2}{l}. \tag{39}$$

Expression (38) coincides with (25), where $\hat{\delta}$ is given by

$$\begin{aligned}\hat{\delta} &= \sqrt{\frac{1}{\pi \hat{\mu}_c \hat{\gamma}_c f}} \\ &= \sqrt{\frac{1}{\pi f \mu_o (\mu'_{rc} - j\mu''_{rc})(\gamma_c + j2\pi f \hat{\varepsilon}_c)}} \\ &= \sqrt{\frac{1}{\pi f \mu_o (\mu'_{rc} - j\mu''_{rc})[\gamma_c + j2\pi f \varepsilon_o (\varepsilon'_{rc} - j\varepsilon''_{rc})]}}. \end{aligned} \tag{40}$$

References

[1] P. J. Dowell, "Effects of eddy currents in transformer windings," *Proc. Inst. Elect. Eng.*, vol. 113, pp. 1387–1394, Aug. 1966.
[2] M. Bartoli, M. K. Kazimierczuk, and A. Reatti, "Predicting the high-frequency ferrite-core inductor performance," presented at the Elect. Manufacturing Coil Winding Conf., Chicago, IL, Sept. 27–29, 1994, pp. 409–413.
[3] ——, "Modeling iron-powder inductors at high frequency," presented at the 29th IEEE Industry Applicat. Soc. Annu. Meeting Tech. Conf., Denver, CO, Oct. 2–5, 1994, pp. 1225–1232.
[4] J. K. Watson, *Applications of Magnetism.* New York: Wiley, 1980.
[5] H. Saotome and Y. Sakaki, "Iron loss analysis of Mn-Zn Ferrite cores," *IEEE Trans. Magnetics*, vol. 33, pp. 728–734, Jan. 1997.
[6] M. Honda, *The Impedance Measurement Handbook.* Hewlett Packard Co., 1994.
[7] G. N. Watson, *A Treatise on the Theory of Bessel Functions.* Cambridge, U.K.: Cambridge Univ. Press, 1966.

Marian K. Kazimierczuk (M'91–SM'91) received the M.S., Ph.D., and D.Sci. degrees in electronics engineering from the Department of Electronics, Technical University of Warsaw, Warsaw, Poland, in 1971, 1978, and 1984, respectively.

He was a Teaching and Research Assistant from 1972 to 1978 and an Assistant Professor from 1978 to 1984 with the Department of Electronics, Institute of Radio Electronics, Technical University of Warsaw, Poland. In 1984, he was a Project Engineer for Design Automation, Inc., Lexington, MA. In 1984–1985, he was a Visiting Professor with the Department of Electrical Engineering, Virginia Polytechnic Institute and State University, VA. Since 1985, he has been with the Department of Electrical Engineering, Wright State University, Dayton, OH, where he is currently a Professor. His research interests are in high-frequency high-efficiency switching-mode tuned power amplifiers, resonant and PWM dc/dc power converters, dc/ac inverters, high-frequency rectifiers, electronic ballasts, magnetics, power semiconductor devices, high-frequency high-efficiency switching-mode power tuned amplifiers, and applied controls. He is the coauthor of the book *Resonant Power Converters* (New York: Wiley, 1995). He has published more than 200 technical papers, 70 of which have appeared in IEEE TRANSACTIONS and JOURNALS.

Dr. Kazimierczuk received the IEEE Harrel V. Noble Award for his contributions to the fields of aerospace, industrial, and power electronics in 1991. He is also a recipient of the 1991 Presidential Award for Faculty Excellence in Research, the 1993 College Teaching Award, the 1995 Presidential Award for Outstanding Faculty Member, and the Brage Golding Distinguished Professor of Research Award from Wright State University. He has been an Associate Editor of the IEEE TRANSACTIONS ON CIRCUITS AND SYSTEMS I and serves as an Associate Editor for the *Journal of Circuits, Systems, and Computers*. He was a member of the Superconductivity Committee of the IEEE Power Electronics Society. He is a member of Tau Beta Pi.

Giuseppe Sancineto was born in Crotone, Italy, in 1968. He received the M.Eng. degree in electrical engineering from the Department of Electrical Engineering, University of Bologna, Bologna, Italy, in 1998, where he is currently working toward the Ph.D. degree.

In 1998, he was a visiting research scholar at the Department of Electrical Engineering, Wright State University, Dayton, OH. His research interests are in the areas of power electronics and electromagnetic compatibility.

Gabriele Grandi was born in Bologna, Italy, in 1965. He received the M.Sc. degree in 1990 (cum laude) and the Ph.D. degree in 1994, both in electrical engineering, from the Department of Electrical Engineering, University of Bologna, Bologna, Italy.

Since 1995, he has been an Assistant Professor (Research Associate) at the Department of Electrical Engineering, University of Bologna, Italy. His research interests are in the areas of modeling, simulation, and design of electronic power converters with particular reference to power conditioning systems. Currently, he studies EMC problems related to electric power apparatus and systems, mainly switching converters and high-frequency circuit models of passive components.

Ugo Reggiani (M'92) received the Laurea degree (cum laude) in electrical engineering from the University of Bologna, Bologna, Italy, in 1969.

He was appointed Assistant at the Department of Engineering, University of Bologna, in 1972, Assistant Professor in 1974, and Full Professor of electrotechnics in 1980. Presently, he is also Head of the Department of Electrical Engineering, University of Bologna. His main research interests concern electromagnetic field theory, electrical machines and drives, electromagnetic compatibility, circuit analysis, and modeling of switched networks.

Dr. Reggiani is a member of the Italian Electrotechnical and Electronic Association (AEI).

Antonio Massarini received the Laurea degree (cum laude) in nuclear engineering and the Ph.D. degree in electrical engineering from the Department of Electrical Engineering, University of Bologna, Bologna, Italy, in 1987 and 1992, respectively.

Since 1993, he has been a Teaching and Research Assistant with the Faculty of Engineering, Department of Engineering Sciences, University of Modena and Reggio Emilia, Modena, Italy. He also cooperates with the Electrical Engineering Department of the University of Bologna, and was a Visiting Professor with the Department of Electrical Engineering, Wright State University, Dayton, OH. His research interests include MHD flow simulation, switched network simulation, magnetics, numerical methods for circuit analysis and design, and switching power converter simulation and design.